# Comparative transcriptomic analysis identifies key genes and regulatory mechanisms of *Passiflora edulis* in response to chilling stress

**Yanyan Wu** [1], **Weihua Huang** [1], **Qinglan Tian** [1], **Jieyun Liu** [1], **Xiuzhong Xia** [2], **Xinghai Yang** [Corresp., 2], **Haifei Mou** [1]

[1] Biotechnology Research Institute, Guangxi Academy of Agricultural Sciences, Nanning, Guangxi, CHINA

[2] Rice Research Institute, Guangxi Academy of Agricultural Sciences, Nanning, Guangxi, CHINA

Corresponding Author: Xinghai Yang
Email address: yangxinghai888@gxaas.net

Chilling stress is an important limiting factor of the growth and development of passion fruit (*Passiflora edulis*) in winter in south China. However, we know little about how passion fruit responds and adapts to cold stress through gene expression regulatory networks. In this study, we performed transcriptome sequencing of Huangjinguo (cold-susceptible) and Tainong1 (cold-tolerant) under normal temperature (NT) and low temperature (LT) conditions, and a total of 80.09 Gb clean reads were generated from 12 samples, resulting in 47,353 unigenes with a total length of 57,343,974 bp. In total, 3,248 and 4,340 differentially expressed genes (DEGs) induced under NT and LT were identified in A1 vs A2 and B1 vs B2. The GO enrichment analysis showed that the DEGs were mainly related to protein phosphorylation, phosphorylation, membrane, catalytic activity. Dissimilarly, more genes were related to plant-pathogen interaction, plant hormone signal transduction and fatty acid metabolism in the KEGG pathway enrichment. After filtering, 12,471 unigenes were used to construct co-expression networks, which were divided into 8 modules, and the brown and yellow modules were related to the cold acclimation. Finally, 32 hub unigenes were obtained in two gene interaction regulatory networks. Moreover, the reliability of cold tolerance-related genes were validated using RT-qPCR. This is the first systematic study of the molecular mechanism of passion fruit cold tolerance, and we found that MAPK signaling pathway, plant hormone signal transduction, starch and sucrose metabolism related genes played a key role in cold acclimation of passion fruit. The results provide theoretical basis and information for the development of passion fruit with increased cold tolerance.

# Title: Comparative transcriptomic analysis identifies key genes and regulatory mechanisms of *Passiflora edulis* in response to chilling stress

Yanyan Wu[1], Weihua Huang[1], Qinglan Tian[1], Jieyun Liu[1], Xiuzhong Xia[2], Xinghai Yang[2*], Haifei Mou[1*]

[1]Biotechnology Research Institute, Guangxi Academy of Agricultural Sciences, Nanning, Guangxi, 530007, China

[2]Rice Research Institute, Guangxi Academy of Agricultural Sciences, Nanning, Guangxi, 530007, China

***Corresponding author**: Xinghai Yang; **Department/Institute**: Rice Research Institute, Guangxi Academy of Agricultural Sciences; **Address**: 174 East Daxue Road, Nanning, Guangxi, 530007, Chian; **E-mail**: yangxinghai514@163.com; Tel: +867713244040; ORCID ID: https://orcid.org/0000-0002-3476-2578.

***Co-corresponding author**: Haifei Mou; **Department/Institute**: Biotechnology Research Institute, Guangxi Academy of Agricultural Sciences; **Address**: 174 East Daxue Road, Nanning, Guangxi, 530007, China; **E-mail**: mhf@gxaas.net; Tel: +86771 3243531

**Abstract**

Chilling stress is an important limiting factor of the growth and development of passion fruit (*Passiflora edulis*) in winter in south China. However, we know little about how passion fruit responds and adapts to cold stress through gene expression regulatory networks. In this study, we performed transcriptome sequencing of Huangjinguo (cold-susceptible) and Tainong1 (cold-tolerant) under normal temperature (NT) and low temperature (LT) conditions, and a total of 80.09 Gb clean reads were generated from 12 samples, resulting in 47,353 unigenes with a total length of 57,343,974 bp. In total, 3,248 and 4,340 differentially expressed genes (DEGs) induced under NT and LT were identified in A1 vs A2 and B1 vs B2. The GO enrichment analysis showed that the DEGs were mainly related to protein phosphorylation, phosphorylation, membrane, catalytic activity. Dissimilarly, more genes were related to plant-pathogen interaction, plant hormone signal transduction and fatty acid metabolism in the KEGG pathway enrichment. After filtering, 12,471 unigenes were used to construct co-expression networks, which were divided into 8 modules, and the brown and yellow modules were related to the cold acclimation. Finally, 32 hub unigenes were obtained in two gene interaction regulatory networks. Moreover, the reliability of cold tolerance-related genes were validated using RT-qPCR. This is the first systematic study of the molecular mechanism of passion fruit cold tolerance, and we found that MAPK signaling pathway, plant hormone signal transduction, starch and sucrose metabolism related genes played a key role in cold acclimation of passion fruit. The results provide theoretical basis and information for the development of passion fruit with increased cold tolerance.

**Key words** Passion fruit, Chilling stres, RNA-seq, WGCNA, Hub genes, RT-qPCR

## Introduction

Passion fruit is a tropical and subtropical fruit tree that is widely planted in south China. Passion fruit has an aromatic smell and high nutritional values: it is rich in sugar, vitamins, and mineral

elements such as calcium, iron, and zinc. Passion fruit is susceptible to LT damage in winter, which can cause big economic loss.

LT is one of the limiting factors for plant growth and development. The leaves are more sensitive to cold damage, and their morphological structure and physiological adaptation are more active under LT stress. The effects of LT on plants can be divided into chilling stress (0-15 $^{o}$C) and freezing stress (<0 $^{o}$C) (Liu et al. 2018). ICE1-CBF-COR is thought to be one of the most important defense pathways in plant against cold stress (Shi et al. 2018). The plants response to LT begins with changing the fluidity of cell membrane. The hardening of cell membrane induced by cold stress can rearrange the cytoskeleton, and cause the activation of calcium channels and increase the level of calcium ions in cytoplasm, causing *COR* gene induction (Guo et al. 2018). CBF can regulate the expression of COR by binding to the CRT/DRE sequence that resides in the promoter region of *COR* gene (Liu et al. 1998; Stockinger et al. 1997). ICE1 (inducer of CBF expression 1) is located upstream of *CBF*, and it is a MYC-like bHLH type transcription factor, which can bind to the recognition site of *CBF3* promoter and regulate its expression (Chinnusamy et al. 2003). MYB15 (Kim et al. 2017), CAMTAs (Doherty et al. 2009) and other transcription factors can also bind to the AP2/ERF binding site of *CBFs* gene to regulate *CBF* expression. In addition, the plant hormones ABA, BR, and GA play an important regulatory role in ICE1-CBF-COR pathway (Ding et al. 2020; Wang et al. 2017).

So far, the systematic study on the cold stress of passion fruit has not been reported. In this study, the RNA-seq was used to analyze gene expression during cold stress in the passion fruit varieties HJG and TN1. The main aims are: (i) analyse the gene expression profile of passion fruit during cold acclimation; (ii) what are the functions of DEGs? (iii) construct regulation network for the interaction of cold tolerance genes of passion fruit; (iv) identify the hub genes that affect the cold acclimation of passion fruit.

## Materials and Methods

### Plant materials

HJG is a cold-sensitive accession, and TN1 is a cold-resistant accession. The cutting seedling

heights ranged from 29 to 38 cm, and the seedlings were transplanted in Nanning experimental field (Guangxi, China, 22.85 ˚N, 108.26 ˚E) on May 25, 2019. The first sampling time was November 25th, 2019, at 10 am in the morning, and the temperature was 25 $^{o}$C. The second sampling time was January 18, 2020, at 10 am in the morning, and the temperature was 7 $^{o}$C. The fresh leaves of passion fruit were snap frozen in liquid nitrogen, and then stored in -80 $^{o}$C freezer. Each sample had three biological replicates. Under NT condition, the three biological replicates of HJG, HJGA1, HJGA2 and HJGA3, are recorded as A1; the three biological replicates of TN1 TN1A1, TN1A2 and TN1A3 are recorded as A2. Under LT condition, three biological replicates of HJG, HJGB1, HJGB2and HJGB3, are denoted as B1; three biological replicates of TN1, TN1B1, TN1B2and TN1B3, are denoted as B2.

**RNA extraction**

Total RNA was extracted with RNAprep Pure kit (Tiangen, Beijing, China) according to the manufacturer's instructions. Nanodrop2000 (Shimadzu, Japan) was used to detect the concentration and purity of the extracted RNA. Agarose gel electrophoresis was used to detect the integrity of the RNA, and Agilent 2100 (Agilent, America) was used to determine the RIN value. A single library requires 1 ug of RNA, with a concentration of $\geq$ 50 ng/μL, and OD 260/280 between 1.8 and 2.2. Magnetic beads (Invitrogen, America) with Oligo (dT) was used to pair with the 3' poly A tail of eukaryotic mRNA, thus isolating mRNA from total RNA for transcriptome analysis.

**Transcriptome sequencing**

The Illumina NovaSeq 6000 platform is designed to sequence short sequences, and the enriched mRNAs were complete RNA sequences. The mRNA needed to be fragmented. Fragmentation buffer could randomly break the mRNA into small fragments of about 300 bp. Under the action of reverse transcriptase, random hexamers were added to reverse-transcribe one-stranded cDNA using mRNA as the template, followed by two-strand synthesis to form stable double-stranded DNA structure. The double-stranded cDNA had a sticky end, which was blunted with the End-Repair Mix. Then, an A base was added at the 3' end to connect the Y-shaped connector. The

sequencing result was imaged, decontaminated, and the adaptors were removed.

**Transcript splicing and functional annotation**

First, we used Trinity (Haas et al. 2013) to splice the transcript fragments to get transcripts, and then used CD-HIT to cluster the transcript sequences to remove redundant sequnces and get all the unigene sequence sets for the subsequent analysis. Bowtie 2 (Salzberg et al. 2012) was used to align the sequencing data to the reconstructed unigene sequence set, the alignment file was mainly used for subsequent unigene quantification and differential expression analysis. The unigene sequences were compared with the NR, Swiss-Prot, TrEMBL, KEGG, GO, Pfam, and KOG databases using BLAST. Then, HMMER was used to align the amino acid sequence of unigene with the Pfam database to obtain the annotation information of unigene.

**Analysis of DEGs**

With the results of comparison to reference transcripts, we obtained the reads number of each gene, and performed TPM (transcripts per million reads) conversion to obtain the expression level of the transcripts. DESeq2 (Love et al. 2014) was used for differential analysis, with the screening threshold FDR (false discovery rate) < 0.05, log2FC (fold change (condition 2/condition 1) for a gene) > 1 or log2FC < -1. The GO enrichment analysis used fisher's test, and we selected the GO term with P (classic Fisher) ≤ 0.05 as the significantly enriched GO term. The significant enrichment analysis on pathways used the KEGG pathway as the unit, and applied hypergeometric test to find the pathways with significantly enriched differential genes. The FDR threshold was set as 0.05.

**Quantitative real-time PCR**

All RT-qPCR assays were carried out in 96-well plates using qTOWER 2.2 Quantitative Real-Time PCR Thermal Cycler (Analytik Jena, Germany). The reaction system included: 10 µl of 2 × TransStart SYBR Green Master Mix (Vazyme, Nanjing, Jiangsu, China), 1 µl of each primer, 1 µl of template cDNA, complemented by ddH2O to 20 µl. The cycle program for product amplification was as follows: 94 °C for 5 min followed by 40 cycles of 94 °C for 30 s (denaturation), 55 °C for 30 s (annealing), and 72 °C for 30 s (extension). Tripricates were set for

each sample. When the reaction was completed, the melting curve was analyzed and specificity of the product was determined based on the melting curve.

**Weighted gene co-expression network analysis**

We followed these steps below for weighted gene co-expression network analysis (GWCNA): (i) screened DEGs for WGCNA cluster analysis; (ii) called the R package to cluster the DEGs; (iii) called ggplot2 in the R package to draw the clustering heat map and histogram of each module; (iv) used the topGO to perform go enrichment analysis on each module; (v) called Fisher-test function in R for KEGG enrichment analysis; (vi) used Cytoscape(Su et al. 2014) to draw network diagram.

**Validation of the cold acclimation-related genes**

We selected 11 genes related to plant hormone signal, fatty acid metabolism and plant-pathogen interaction in GO and KEGG database, and 4 hub genes in WGCNA for validation. The primers were designed using Primer3 （Table S1）. Using *HIS* as the reference gene (Liu et al. 2017A), RT-qPCR was used to analyze the expression level of 15 genes in B1 and B2. The relative gene expression level was calculated by reference to the $2^{-\Delta\Delta Ct}$ method (Livak et al. 2001).

**Results**

**Quality control and assembly of passion fruit transcriptome sequences**

The raw image files of the sequencing data were converted to unfiltered raw reads by base recognition analysis. After decontamination and adaptor removal, 533,935,574 raw reads were obtained from 12 samples, with 80.09 Gb clean reads and 6.67 Gb per sample on average. The Q30 base percentage was 93.22% and GC content was 44.64% (Table 1). The quality control of passion fruit transcriptome sequencing was good, and the quality of cleaned data was acceptable for subsequent analysis.

We used Trinity to splice the transcript fragments to obtain 211,874 transcript sequences, and then used CD-HIT to cluster the sequences and remove the redundant sequences, which yielded 47,353 unigenes. The total length of unigenes was 57,343,974 bp, N50 was 2,368 bp, N90 was 450 bp, with an average length of 1,211 bp. After that, Bowtie2 was used to align the sequences

of each sample to the unigene sequence set, with an average alignment ratio of 77.89% (Table 2).

**Gene function annotation**

BLAST (E-value <1e-5) was used to compare all the unigenes to NR, Swiss-Prot, TrEMBL, KEGG, GO, Pfam, and KOG databases, and 47,353 unigenes acquired annotation information (Table 3). The number of annotated unigenes in NR and TrEMBL was the largest, which were 46,369 and 46,323 respectively. In the GO database, 17,123 unigenes were annotated and matched to three major categories: molecular function (MF), cell composition (CC) and biological process (BP). In BP, metabolic process contained the most annotated unigenes (4,350), followed by cellular process (2,191); in CC, membrane part had the largest number of annotated unigenes (1,270), followed by cell part (890); In MF, binding contained the most annotated unigenes (7,367), followed by catalytic activity (5,715) (Fig. 1).

In the KOG database, 23,164 unigenes were annotated. They were clustered into 25 functional categories, and the number of genes in different functional categories was significantly different. The number of unigenes related to signal transduction mechanisms was the most (2,439), followed by posttranslational modification, protein turnover, chaperones (2,138), and the least was cell motility (8) (Fig. 2).

In the KEGG database, 16,086 unigenes were annotated. According to the functions, these unigenes were divided into 9 categories: antineoplastic, cellular processes, environmental information processing, genetic information processing, human diseases, metabolism, organizational systems and viral and specific types, in which the number of unigenes involved in metabolism was the largest (10,045), followed by organismal systems (4,505), and antineoplastic had the least unigenes (311) (Fig. 3).

**Gene expression analysis**

By comparing the TPM density distribution of transcripts in different samples, we could check the overall TPM distribution in different samples (Fig. S1).

The correlation of gene expression levels between samples is an important indicator for testing the reliability of experiments and the rationality of sample selection. Correlation coefficient

closer to 1 indicates higher similarity of the expression patterns. We used the TPM value of unigenes to calculate the correlation coefficient of each two samples (Fig. S2). The correlation coefficient between the three biological replicates was 0.87 in HJGA, 0.98 in TN1A, 0.96 in HJGB, 0.99 in TN1B, and the average correlation coefficient value was 0.95, indicating that the reproducibility of this study was good and the experimental results were reliable.

**Differential expressed gene analysis**

DESeq2 software was used to perform differential expression analysis of unigenes between samples or groups. Through certain standardized processing and screening conditions, we obtained differentially expressed unigenes between groups. The default parameter was P-adjust <0.05 & |log2FC|> = 1. There were 1,182 upregulated unigenes, and 2,066 downregulated unigenes when comparing A1 to A2; and there were 2,137 upregulated unigenes and 2,203 downregulated unigenes when comparing B1 to B2, indicating that the number of DEGs between HJG and TN1 was increased by 33.6% under cold damage (1,092), and 87.5% (955) were up-regulation (Fig. 4).

Cluster analysis of gene expression can intuitively reflect the level of gene expression and expression patterns in multiple samples. We used the DEGs to perform cluster analysis on A1 vs A2 (Fig. 5a) and B1 vs B2 (Fig. 5b), with a total of 12 samples. The results showed that the difference between the three biological replicates of each group was small, which again confirmed the rationality of sample selection.

**Functional enrichment analysis of DEGs**

We performed Fisher's test on GO enrichment analysis, and $P \leq 0.05$ was considered as the significantly enriched GO term. In the BP of A1 vs A2, there were more genes related to metabolic process (542), oxidation-reduction process (156), protein phosphorylation (92), carbohydrate metabolic process (73), organic substance catabolic process (40), and catabolic process (40); in CC, more genes were enriched in extracellular region (10), apoplast (8), cell wall (8), and external encapsulating structure (8); in MF, there were more genes enriched in catalytic activity (634), transferase activity (228), oxidoreductase activity (167), metal ion binding (146),

cation binding (146), and transition metal ion binding (110) (Table S2).

In the BP of B1 vs B2, there were more genes enriched in oxidation-reduction process (187), phosphate-containing compound metabolic process (171), phosphorus metabolic process (171), macromolecule modification (170), cellular protein modification process (169), and protein modification process (169); in CC, more genes were enriched in membrane (213), intrinsic component of membrane (99), and integral component of membrane (97); in MF, there were more genes enriched in catalytic activity (837), transferase Activity (326), cation binding (202), metal ion binding (201), oxidoreductase activity (198), phosphotransferase activity, and alcohol group as acceptor (165) (Table S3).

The GO terms with $P > 0.05$ in A1 vs A2 and $P \leq 0.05$ in B1 vs B2 were selected for analysis. In BP, more genes were enriched in protein phosphorylation (61), phosphorylation (61), response to stimulus (35), lipoid metabolic process (19), response to chemical (13); in CC, there were more genes enriched in membrane (73), intrinsic component of membrane (29), and integral component of membrane (28); in MF, more genes were enriched catalytic activity, acting on a protein (77), transferase activity, transferring phosphorus-containing groups (70), kinase activity (67), phosphotransferase activity, alcohol group as acceptor (67), and protein kinase activity (62) (Table S4).

In cells, different genes coordinate together to perform their biological functions. The pathway enrichment analysis can reveal the main metabolic pathways and signal transduction pathways in which the DEGs were involved. In A1 vs A2, more genes were enriched in ribosome (42), carbon metabolism (39), biosynthesis of amino acids (30), starch and sucrose metabolism (21), and cysteine and methionine metabolism (20); in B1 vs B2, more genes were enriched in plant hormone signal transduction (31), plant-pathogen interaction (27), fatty acid metabolism (21), cysteine and methionine metabolism (20) (Fig. 6a). In the pathways with $P > 0.05$ in A1 vs A2 and $P \leq 0.05$ in B1 vs B2, there were more genes enriched in plant-pathogen interaction (17), plant hormone signal transduction (14), and fatty acid metabolism (8) ( Fig. 6b).

**WGCNA analysis on DEGs**

After background correction and normalization of the unigenes expression data, we filtered out the abnormal genes and genes with small variations, and obtained 12,471 highly expressed unigenes. In this study, when the soft threshold was 16 (Fig. S3), the gene topology matrix expression network was closest to the scale-free distribution. A gene cluster tree was constructed based on the correlation between genes, and each branch corresponded to a cluster of gene sets with highly correlated expression levels (Fig. S4a).

According to the standard of mixed dynamic shear, the gene modules were classified and the eigenvector of each module was calculated. The modules close to each other were merged, and 8 co-expression modules were obtained (Fig. S4b). Each module used different colors to represent the clustered genes. The turquoise module had the most clustered genes (4,171), the red module contained the fewest (81), and the grey module contained the unigenes that couldn't be included in any module.

The differentially expressed unigenes were used to draw the heat map of each module in the 4 sample groups. The brown and yellow modules showed less changes in differential genes between the early and late HJG, but showed larger changes in differential genes between early and late TN1 (Fig.7), which is consistent with the cold resistance feature of TN1. Therefore, we selected the unigenes of these two modules for in-depth GO enrichment analysis and pathway analysis.

In the brown module, the GO terms significantly enriched in BP were cellular macromolecule metabolic process (GO: 0044260), phosphate-containing compound metabolic process (GO: 0006796), phosphorus metabolic process (GO: 0006793), protein phosphorylation (GO: 0006468), stimulus (GO: 0050896), etc., a total of 44 GO terms; the GO terms significantly enriched in CC were transferase complex (GO: 1990234), riboflavin synthase complex (GO: 0009349), photosystem I reaction center (GO: 0009538), and photosystem I ( GO: 0009522), a total of 4 GO terms; the GO terms significantly enriched in MF were ion binding (GO: 0043167), metal ion binding (GO: 0046872), cation binding (GO: 0043169), phosphotransferase activity, alcohol group as acceptor (GO: 0016773), kinase activity (GO: 0016301), etc., a total of 42 GO

271 terms (Table S5). There were 30 significantly enriched pathways, including plant hormone signal
272 transduction (ko04075), MAPK signaling pathway (ko04010), starch and sucrose metabolism
273 (ko00500) and other pathways that might be involved in cold damage (Fig. 8).
274 In the yellow module, the GO terms significantly enriched in BP were cellular process (GO:
275 0009987), macromolecule modification (GO: 0043412), phosphorus metabolic process (GO:
276 0006793), cellular protein modification process (GO: 0006464), protein modification process (
277 GO: 0036211), etc., a total of 30 GO terms; the GO terms significantly enriched in CC were cell
278 periphery (GO: 0071944), photosystem (GO: 0009521), photosynthetic membrane (GO:
279 0034357), thylakoid (GO: 0009579), extracellular region (GO : 0005576), etc., a total of 15 GO
280 terms; the GO terms significantly enriched in MF were 3-deoxy-7-phosphoheptulonate synthase
281 activity (GO: 0003849), alkylbase DNA N-glycosylase activity (GO: 0003905), DNA-3-
282 methyladenine glycosylase activity (GO: 0008725), DNA N-glycosylase Activity (GO: 0019104),
283 method adenosyltransferase activity (GO: 0004478), etc., a total of 32 GO terms (Table S6). The
284 significantly enriched pathways included biosynthesis of amino acids (ko01230), plant hormone
285 signal transduction (ko04075), ABC transporters (ko02010), starch and sucrose metabolism
286 (ko00500), folate biosynthesis (ko00790) and other pathways that might be related to cold
287 damage (Fig. 9).
288 We used Cytoscape to draw network diagram in the brown and yellow module, and got 19 hub
289 unigenes, mainly related to MAPK signaling pathway, plant hormone signal transduction, starch
290 and sucrose metabolism, fatty acid biosynthesis and photosynthesis in the brown module (Fig.
291 10a). In the yellow module, we get 13 hub unigenes, mainly related to plant hormone signal
292 transduction, MAPK signaling pathway, starch and sucrose metabolism and fatty acid
293 degradation (Fig. 10b).
294 **Validation of gene expression changes during cold acclimation**
295 We used the RT-qPCR method to validate the expression level of 15 unigenes identified from
296 RNA-seq. The results showed that the RT-qPCR expression patterns of the 15 unigenes were
297 consistent with RNA-seq analysis (Fig. 11, Table S7). RT-qPCR analysis showed that there were

9 unigenes fold-change≥2 or ≤0.5. Comparison with B1 and B2, 12 genes had TPM values g≥2 or ≤0.5. 9 out 12 DEGs could be validated via RT-qPCR, and the results of DEGs analysis were highly reliable.

**Discussions**

In this study, the number of annotated unigenes in NR and TrEMBL were higher, which were 46,369 and 46,323, respectively. This was likely due to the larger number of genes collected in these two databases, including many proteins with unknown functions. 17,123 unigenes were annotated in the GO database, and there were more genes related to metabolic process, cell part, and binding; in the KOG database, there were more unigenes related to signal transduction mechanisms, posttranslational modification, protein turnover, and chaperones; in KEEG database, more unigenes were related to metabolism, which was similar to the result in GO database, while in KOG, the unigenes related to signal transduction mechanisms were more.

Compared with FPKM, the TPM value could reflect the reads ratio of specific unigene, so that this value can be directly compared between samples. After the cold injury of passion fruit, the number of down-regulated DEGs did not change much, but the number of up-regulated differential unigenes were 955, indicating that the up-regulation of multiple DEGs might be related to the cold domestication of passion fruit.

We selected the DEGs with $P > 0.05$ in group A and $P \leq 0.05$ in group B for GO enrichment analysis, and found there were more genes related to protein phosphorylation, response to stimulus, lipid metabolic process, protein kinase activity, catalytic activity (acting on a protein); in pathway analysis, more genes were related to plant hormone signal transduction, plant-pathogen interaction, fatty acid metabolism, cysteine and methionine metabolism. Under the condition of cold stimulation, the transmembrane protein COLD1 senses the cold signal through an unknown mechanism (Ma et al. 2015), and then interacts with G protein (Gα) to activate plasma membrane calcium channels, which promotes the increase of intracellular calcium concentration (Yuan et al. 2018A). The damage to cell membranes at LT is mainly caused by the unsaturation of fatty acids in the cells and lipid peroxidation (Krishnan et al. 2008). When plants

are subjected to LT stress, fatty acid dehydrogenase regulates fatty acid unsaturation to increase the fluidity of cell membrane, thereby improving the cold-resistance of plant (Upchurch 2008; He et al. 2015). The change of malondialdehyde content caused by lipid peroxidation is negatively correlated with plant cold resistance (Kim et al. 2011). Protein phosphorylation is also a type of post-translational regulation during the cold acclimation of plant. Under LT condition, CRPK1 is activated and phosphorylate 14-3-3λ, then the phosphorylated 14-3-3λ enters nucleus from the cytoplasm and degrades CBFs via direct interaction in *Arabidopsis* (Liu et al. 2017B). Mitogen-activated protein kinase (MAPK) plays an important role in signal transduction, and is also essential for regulating the cold response of plants. Zhao et al. found that under LT treatment, the phosphorylation levels of MPK3, MPK4 and MPK6 were significantly increased (Zhao et al. 2017); moreover, MPK3 and MPK6 could interact with ICE1 to participate in low-temperature response (Li et al.). Zhang et al. found that the phosphorylated OsICE1 could promote *OsTPP1* transcription and induce the production of large amounts of trehalose, thereby improving the cold resistance of rice (Zhang et al. 2017).

Abscisic acid (ABA) is an important plant hormone that regulates plant growth and stoma closure, especially when plants are subjected to environmental stress. The core ABA signaling pathway consists of a series of PYR/PYL/RCAR receptor families, an evolutionary PP2C family as negative regulators and co-receptors, and a member of positive effector subgroup III, SnRK2s (Wang et al. 2018). In addition, BR, GA, JA, ethylene, auxin, CK, and melatonin play important regulatory roles in the ICE–CBF–COR pathway (Wang et al. 2017). The interaction between plants and pathogens also plays a role in stress resistance. Overexpression and ectopic expression of *CaPIF1* in tomato led to cold tolerance and disease resistance (Seong es et al. 2007). Wu et al. also showed that plant–pathogen interaction pathways were linked to the cold acclimation in *Vitis amurensis* grapevine (Wu et al. 2014).

The WGCNA analysis indicated that two modules could be related to the cold acclimation of passion fruit. The two modules contained a different number of cold stress-related hub genes, and they all contained plant hormone signal transduction, MAPK signaling pathway, starch and

sucrose metabolism and fatty acid metabolism related genes. Endogenous hormones play an important role in inducing stress to produce defensive adaptation, and many hub genes were related to auxin and ABA in this study. Auxin plays a trigger in plant growth and development. In rice, ROC1 can regulate *CBF1*, and auxin can affect ROC1 levels (Dou et al. 2016). ABA is used as an important signal molecule and the most important stress signal in hormones, and it can mediate the signal transduction pathway to cold stress and increase the tolerance of cold stress (Yuan et al. 2018B). *MKK2* induces *COR* expression to improve the cold tolerance of plants. *OsMKK6* and *OsMPK3* constitute a moderately low-temperature signalling pathway and regulate cold stress tolerance in rice (Xie et al. 2012). *MAPK3*/*6* phosphorylates ICE1 and promotes its degradation, negatively regulating the cold tolerance mechanism in *Arabidopsis thaliana* (Li et al.; Zhao et al. 2017). In the process of cold acclimation in plants, starch intensifies hydrolysis, the content of soluble sugar increases, the concentration of cell fluid increases, the freezing point is lowered, and the excessive dehydration of cells is reduced (Yue et al. 2015; Krasensky j 2012). Liu et al. found that the overexpression of the wheat *trehalose 6-phosphate synthase 11* gene enhanced cold tolerance in *Arabidopsis thaliana* (Liu et al. 2019). Compared with the yellow module, the photosynthesis pathway of the brown module plays an important role in the cold acclimation of passion fruit. C3 and C4 plants adjust their photosynthetic characteristics to suit their growth temperature (Yamori et al. 2014). Zhang et al. found that BR could reduce the damage caused by cold damage by maintaining the stability of the leaf structure, shape and function, thereby improving the photosynthetic potential of tung (Zhang et al. 2020).

## Conclusions

In this study, 12 passion fruit samples were sequenced and yielded 80.09 Gb clean reads, with 6.67 Gb per sample on average. Atotal of 47,353 unigenes were obtained, and 46,369 and 46,323 unigenes were annotated in NR and TrEMBL database which have the most annotated unigenes. In the GO database, 17,123 unigenes were annotated that are involved in metabolic process, membrane part, binding; in the KOG database, the most unigenes were clustered into

signal transduction mechanisms and posttranslational modification; the most unigenes were involved in metabolism. A total of 3,248 and 4,340 DEGs in A1 vs A2 and B1 vs B2 were identified which are involved in protein phosphorylation, phosphorylation, response to stimulus, membrane, catalytic activity, transferase activity, kinase activity and phosphotransferase activity in GO, and plant-pathogen interaction, plant hormone signal transduction and fatty acid metabolism in KEGG. The WGCNA results showed that brown and yellow modules are highly related to the cold acclimation of passion fruit. We got 32 hub genes in the two modules, which are related to MAPK signaling pathway, plant hormone signal transduction, starch and sucrose metabolism, fatty acid metabolism, and photosynthesis. These findings provide an understanding of the molecular regulation mechanism and facilitate the genetic improvement of cold tolerance in passion fruit.

**Acknowledgments**

The authors thank to Dr. Yinghua Pan for help.

**ADDITIONAL INFORMATION AND DECLARATIONS**

**Funding**

This work was supported by Guangxi Natural Science Foundation of China (2018GXNSFBA281024, 2019GXNSFAA245002), Guangxi's Ministry of Science and Technology (AB18294007), Guangxi Academy of Agricultural Sciences (2018YT19, TS2016010). The funding bodies had no role in the design of the study and collection, analysis, and interpretation of data and in writing the manuscript.

**Grant Disclosures**

The following grant information was disclosed by the authors:

Guangxi Natural Science Foundation of China: 2018GXNSFBA281024, 2019GXNSFAA245002.

Guangxi's Ministry of Science and Technology: AB18294007.

Guangxi Academy of Agricultural Sciences: 2018YT19, TS2016010.

**Conflicts of interest**

The authors declare no competing interests.

**Author Contributions**

•Haifei Mou and Xinghai Yang conceived and designed the experiments,

•Yanyan Wu analyzed the data and wroted this manuscript,

•Weihua Huang conducted all field trials and collectd the samples,

•Qinglan Tian extracted mRNA and performed qPCR analysis,

•Jieyun Liu designed the primers,

•Xiuzhong Xia prepared the figures,

•Xinghai Yang revised the manuscript. All authors read and approve the paper.

**Availability of data**

The RNA-seq data that support the findings of this study have been deposited to National Center for Biotechnology Information (NCBI) Sequence Read Archive (SRA) with the accession code PRJNA634206 [https://www.ncbi.nlm.nih.gov/sra/PRJNA634206].

# References

**Chinnusamy V, Ohta M, Kanrar S, Lee BH, Hong X, Agarwal M, Zhu JK. 2003.** ICE1: a regulator of cold-induced transcriptome and freezing tolerance in Arabidopsis. Genes Dev **17**: 1034-1054.

**Ding Y, Shi Y, Yang S. 2020.** Molecular regulation of plant responses to environmental temperatures. Mol Plant **13**: 544-564.

**Doherty CJ, Van buskirk HA, Myers SJ, Thomashow MF. 2009.** Roles for Arabidopsis CAMTA transcription factors in cold-regulated gene expression and freezing tolerance. Plant Cell **21**: 972-984.

**Dou M, Cheng S, Zhao B, Xuan Y, Shao M. 2016.** The indeterminate domain protein ROC1 regulates chilling tolerance via activation of DREB1B/CBF1 in rice. Int J Mol Sci **17**: 233.

**Guo X, Liu D, Chong K. 2018.** Cold signaling in plants: Insights into mechanisms and regulation. J Integr Plant Biol **60**: 745-756.

**Haas BJ, Papanicolaou A, Yassour M, Grabherr M, Blood PD, Bowden J, Couger MB, Eccles D, Li B, Lieber M, Macmanes MD, Ott M, Orvis J, Pochet N, Strozzi F, Weeks N, Westerman R, William T, Dewey CN, Henschel R, Leduc RD, Friedman N, Regev A. 2013.** De novo transcript sequence reconstruction from RNA-seq using the Trinity

platform for reference generation and analysis. Nat Protoc **8**: 1494-1512.
**He J, Yang Z, Hu B, Ji X, Wei Y, Lin L, Zhang Q. 2015.** Correlation of polyunsaturated fatty acids with the cold adaptation of Rhodotorula glutinis. Yeast **32**: 683-690.
**Kim SI, Tai TH. 2011.** Evaluation of seedling cold tolerance in rice cultivars: a comparison of visual ratings and quantitative indicators of physiological changes. Euphytica **178**: 437-447.
**Kim SH, Kim HS, Bahk S, An J, Yoo Y, Jy K, Chung WS. 2017.** Phosphorylation of the transcriptional repressor MYB15 by mitogen-activated protein kinase 6 is required for freezing tolerance in Arabidopsis. Nucleic Acids Res **45**: 6613-6627.
**Krasensky j JC. 2012.** Drought, salt, and temperature stress-induced metabolic rearrangements and regulatory networks. J Exp Bot **63**: 1593-1608.
**Krishnan N, Dickman MB, Becker DF. 2008.** Proline modulates the intracellular redox environment and protects mammalian cells against oxidative stress. Free Radic Biol Med **44**: 671-681.
**Li H, Ding YL, Shi YT, Zhang XY, Zhang SQ, Gong ZZ, Yang SH.** MPK3- and MPK6-mediated ICE1 phosphorylation negatively regulates ICE1 stability and freezing tolerance in Arabidopsis. Dev Cell **43**: 630-642.
**Liu Q, Kasuga M, Sakuma Y, Abe H, Miura S, Yamaguchi-shinozaki K, Shinozaki K. 1998.** Two transcription factors, DREB1 and DREB2, with an EREBP/AP2 DNA binding domain separate two cellular signal transduction pathways in drought- and low-temperature-responsive gene expression, respectively, in Arabidopsis. Plant Cell **10**: 1391-1406.
**Liu S, Li AD, Chen CH, Cao GJ, Zhang LM, Guo CY, Xu M. 2017A.** De Novo Transcriptome Sequencing in Passiflora edulis Sims to Identify Genes and Signaling Pathways Involved in Cold Tolerance. Forests **8**: 435.
**Liu Z, Jia Y, Ding Y, Shi Y, Li Z, Guo Y, Gong Z, Yang S. 2017B.** Plasma membrane CRPK1-mediated phosphorylation of 14-3-3 proteins induces their nuclear import to fine-tune CBF signaling during cold response. Mol Cell **66**: 117-128.
**Liu J, Shi Y, Yang S. 2018.** Insights into the regulation of C-repeat binding factors in plant cold signaling. J Integr Plant Biol **60**: 780-795.
**Liu X, Fu L, Qin P, Sun Y, Liu J, Wang X. 2019.** Overexpression of the wheat trehalose 6-phosphate synthase 11 gene enhances cold tolerance in Arabidopsis thaliana. Gene **710**: 210-217.
**Livak KJ, Schmittgen TD. 2001.** Analysis of relative gene expression data using real-time quantitative PCR and the 2(-Delta Delta C(T)) Method. Methods **25**: 402-408.
**Love MI, Huber W, Anders S. 2014.** Moderated estimation of fold change and dispersion for RNA-seq data with DESeq2. Genome Biol **15**: 550.
**Ma Y, Dai X, Xu Y, Luo W, Zheng X, Zeng D, Pan Y, Lin X, Liu H, Zhang D, Xiao J, Guo X, Xu S, Niu Y, Jin J, Zhang H, Xu X, Li L, Wang W, Qian Q, Ge S, Chong K. 2015.** COLD1 confers chilling tolerance in rice. Cell **160**: 1209-1221.
**Salzberg SL, Langmead B. 2012.** ast gapped-read alignment with Bowtie 2. Nat Methods **9**: 357-359.
**Seong es BS, Cho hs CD. 2007.** Induction of enhanced tolerance to cold stress and disease by

overexpression of the pepper CAPIF1 gene in tomato. Physiol Plant **129**: 555-566.
**Shi Y, Ding Y, Yang S. 2018.** Molecular regulation of CBF signaling in cold acclimation. Trends Plant Sci **23**: 623-637.
**Stockinger EJ, Gilmour SJ, Thomashow MF. 1997.** Arabidopsis thaliana CBF1 encodes an AP2 domain-containing transcriptional activator that binds to the C-repeat/DRE, a cis-acting DNA regulatory element that stimulates transcription in response to low temperature and water deficit. Proc Natl Acad Sci U S A **94**: 1035-1040.
**Su G, Morris JH, Demchak B, Bader GD. 2014.** Biological network exploration with Cytoscape 3. Curr Protoc Bioinformatics **8**: 8.13.1–8.1.
**Upchurch RG. 2008.** Fatty acid unsaturation, mobilization, and regulation in the response of plants to stress. Biotechnol Lett **30**: 967-977.
**Wang DZ, Jin YN, Ding XH, Wang WJ, Zhai SS, Bai LP, Guo ZF. 2017.** Gene regulation and signal transduction in the ICE-CBF-COR signaling pathway during cold stress in plants. Biochemistry (Mosc) **82**: 1103-1117.
**Wang H, Tang J, Liu J, Hu J, Liu J, Chen Y, Cai Z, Wang X. 2018.** Abscisic acid signaling inhibits brassinosteroid signaling through dampening the dephosphorylation of BIN2 by ABI1 and ABI2. Mol Plant **11**: 315-325.
**Wu J, Zhang Y, Yin L, Qu J, Lu J. 2014.** Linkage of cold acclimation and disease resistance through plant-pathogen interaction pathway in Vitis amurensis grapevine. Funct Integr Genomics **14**: 741-755.
**Xie G, Kato H, Imai R. 2012.** Biochemical identification of the OsMKK6-OsMPK3 signalling pathway for chilling stress tolerance in rice. Biochem J **443**: 95-102.
**Yamori W, Hikosaka K, Way DA. 2014.** Temperature response of photosynthesis in C3, C4, and CAM plants: temperature acclimation and temperature adaptation. Photosynth Res **119**: 101-117.
**Yuan P, Du L, Poovaiah BW. 2018A.** Ca2+/Calmodulin-dependent AtSR1/CAMTA3 plays critical roles in balancing plant growth and immunity. Int J Mol Sci **19**: E1764.
**Yuan P, Yang T, Poovaiah BW. 2018B.** Calcium signaling-mediated plant response to cold stress. Int J Mol Sci **19**: E3896.
**Yue C, Cao HL, Wang L, Zhou YH, Huang YT, Hao XY, Yc W, Wang B, Yang YJ, Wang XC. 2015.** Effects of cold acclimation on sugar metabolism and sugar-related gene expression in tea plant during the winter season. Plant Mol Biol **88**: 591-608.
**Zhang Z, Li J, Li F, Liu H, Yang W, Chong K, Xu Y. 2017.** OsMAPK3 phosphorylates OsbHLH002/OsICE1 and inhibits its ubiquitination to activate OsTPP1 and enhances rice chilling tolerance. Dev Cell **43**: 731-745.
**Zhang F, Lu K, Gu Y, Zhang L, Li W, Li Z. 2020.** Effects of low-temperature stress and brassinolide application on the photosynthesis and leaf structure of tung tree seedlings. Front Plant Sci **10**: 1767.
**Zhao C, Wang P, Si T, Hsu CC, Wang L, Zayed O, Yu Z, Zhu Y, Dong J, Tao W, Zhu JK. 2017.** MAP Kinase Cascades Regulate the Cold Response by Modulating ICE1 Protein Stability. Dev Cell **43**: 618-629.

518

## Table 1(on next page)

Statistical results of transcriptome sequencing.

Table 1 Statistical results of transcriptome sequencing.

| Sample | Reads number | Total base (bp) | Q30 (%) | GC content (%) |
|---|---|---|---|---|
| HJGA1 | 46599672 | 6989950800 | 93.02 | 45.36 |
| HJGA2 | 44522400 | 6678360000 | 93.08 | 44.49 |
| HJGA3 | 46642622 | 6996393300 | 93.23 | 45.31 |
| TNA1 | 47166760 | 7075014000 | 93.18 | 45.23 |
| TNA2 | 43505726 | 6525858900 | 93.31 | 44.33 |
| TNA3 | 45058566 | 6758784900 | 93.16 | 43.83 |
| HJGB1 | 44758052 | 6713707800 | 93.34 | 43.83 |
| HJGB2 | 43843522 | 6576528300 | 93.43 | 44.70 |
| HJGB3 | 39087142 | 5863071300 | 93.14 | 43.37 |
| TNB1 | 49306634 | 7395995100 | 93.31 | 45.51 |
| TNB2 | 44267228 | 6640084200 | 93.17 | 44.87 |
| TNB3 | 39177250 | 5876587500 | 93.27 | 44.89 |

## Table 2(on next page)

Sequencing data mapped to unigene set.

Table 2 Sequencing data mapped to unigene set.

| Sample | Pair reads | Aligned concordantly 0 times | Aligned concordantly exactly 1 time | Aligned concordantly >1 times | Total alignment ratio（%） |
|---|---|---|---|---|---|
| HJGA1 | 23299836 | 6183910 | 15486803 | 1629123 | 83.19 |
| HJGA2 | 22261200 | 6461646 | 14313504 | 1486050 | 81.73 |
| HJGA3 | 23321311 | 7002139 | 14768806 | 1550366 | 81.04 |
| TNA1 | 23583380 | 8597970 | 13025983 | 1959427 | 75.69 |
| TNA2 | 21752863 | 7919003 | 11974898 | 1858962 | 75.79 |
| TNA3 | 22529283 | 7817813 | 12764435 | 1947035 | 77.11 |
| HJGB1 | 22379026 | 6946292 | 14131411 | 1301323 | 78.91 |
| HJGB2 | 21921761 | 6859052 | 13821399 | 1241310 | 78.45 |
| HJGB3 | 19543571 | 5267390 | 12862365 | 1413816 | 81.72 |
| TNB1 | 24653317 | 9000336 | 13737412 | 1915569 | 74.21 |
| TNB2 | 22133614 | 8908390 | 11548761 | 1676463 | 70.83 |
| TNB3 | 19588625 | 6676080 | 11320050 | 1592495 | 75.95 |

## Table 3(on next page)

Unigenes were annotated to 7 databases.

Table 3 Unigenes were annotated to 7 databases.

| Database | Annotated number | Annotated ratio (%) |
|---|---|---|
| GO | 17123 | 36.16 |
| KEGG | 16086 | 33.97 |
| KOG | 23164 | 48.92 |
| NR | 46369 | 97.92 |
| Pfam | 29091 | 61.43 |
| Swiss-Prot | 33337 | 70.40 |
| TrEMBL | 46323 | 97.82 |
| Total | 47353 | 100 |

# Figure 1

GO function classification diagram of unigenes. The x-axis indicates the secondary classification terms of GO; the y-axis indicates the number of unigenes in this secondary classification out of the total annotated unigenes.

The x-axis indicates the secondary classification terms of GO; the y-axis indicates the number of unigenes in this secondary classification out of the total annotated unigenes.

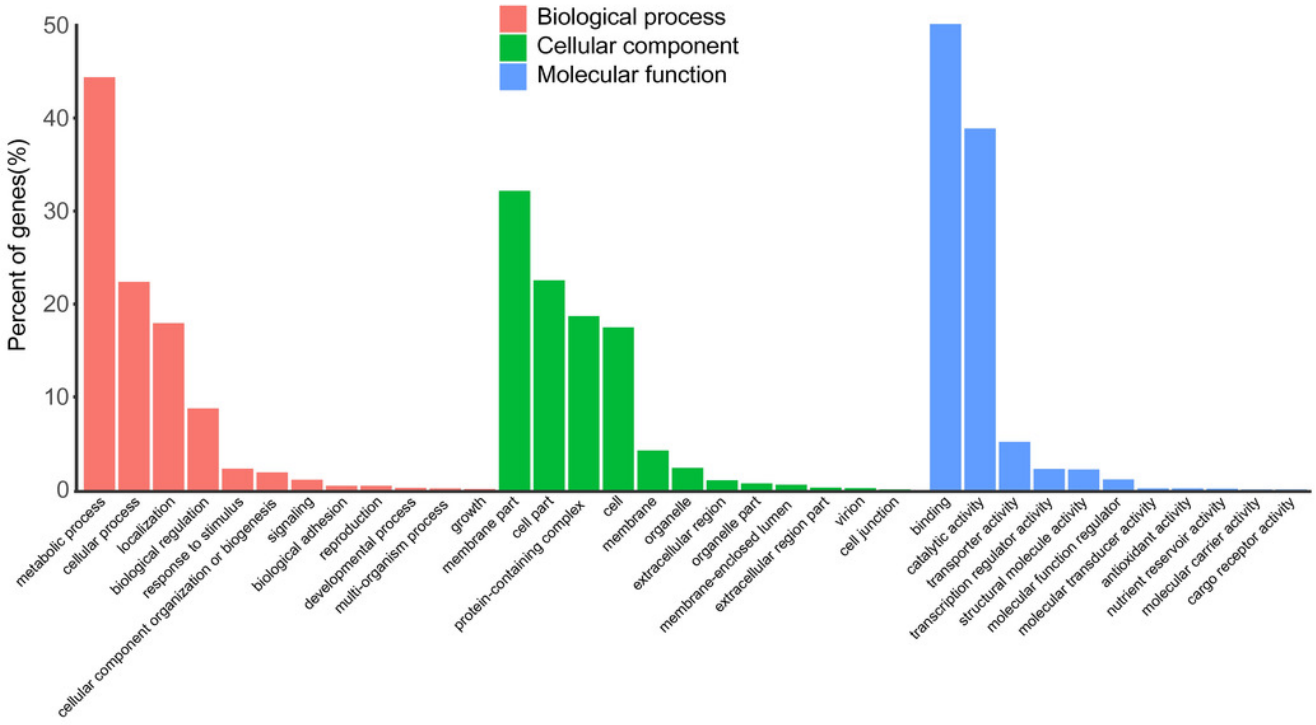

# Figure 2

KOG functional annotation distribution of unigenes.

The x-axis indicates the nuber unigens; the y-axis indicates the name of 25 groups.

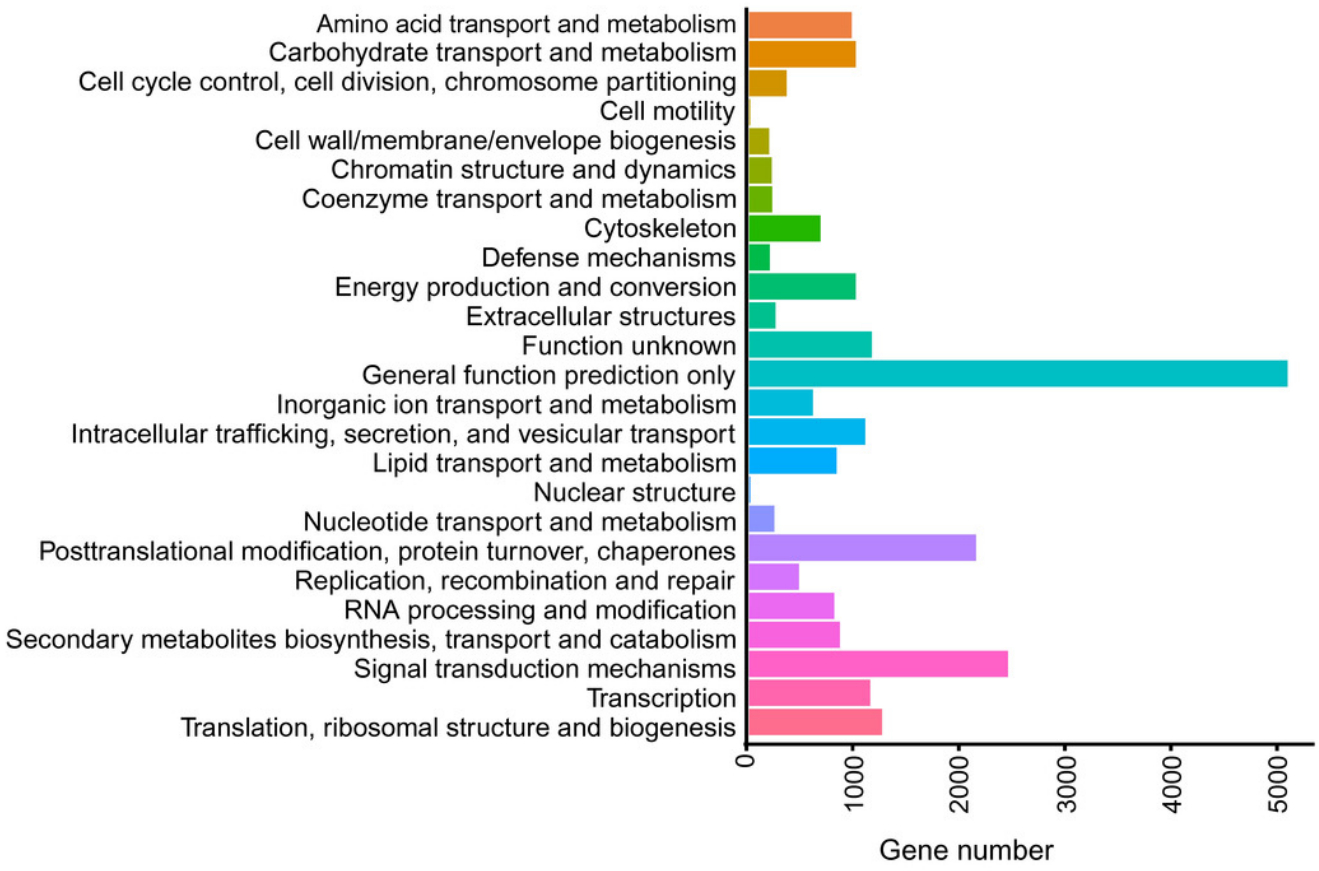

# Figure 3

KEGG classification of unigenes.

The x-axis indicates the number of unigenes in the pathway; the y-axis indicates KEGG pathways.

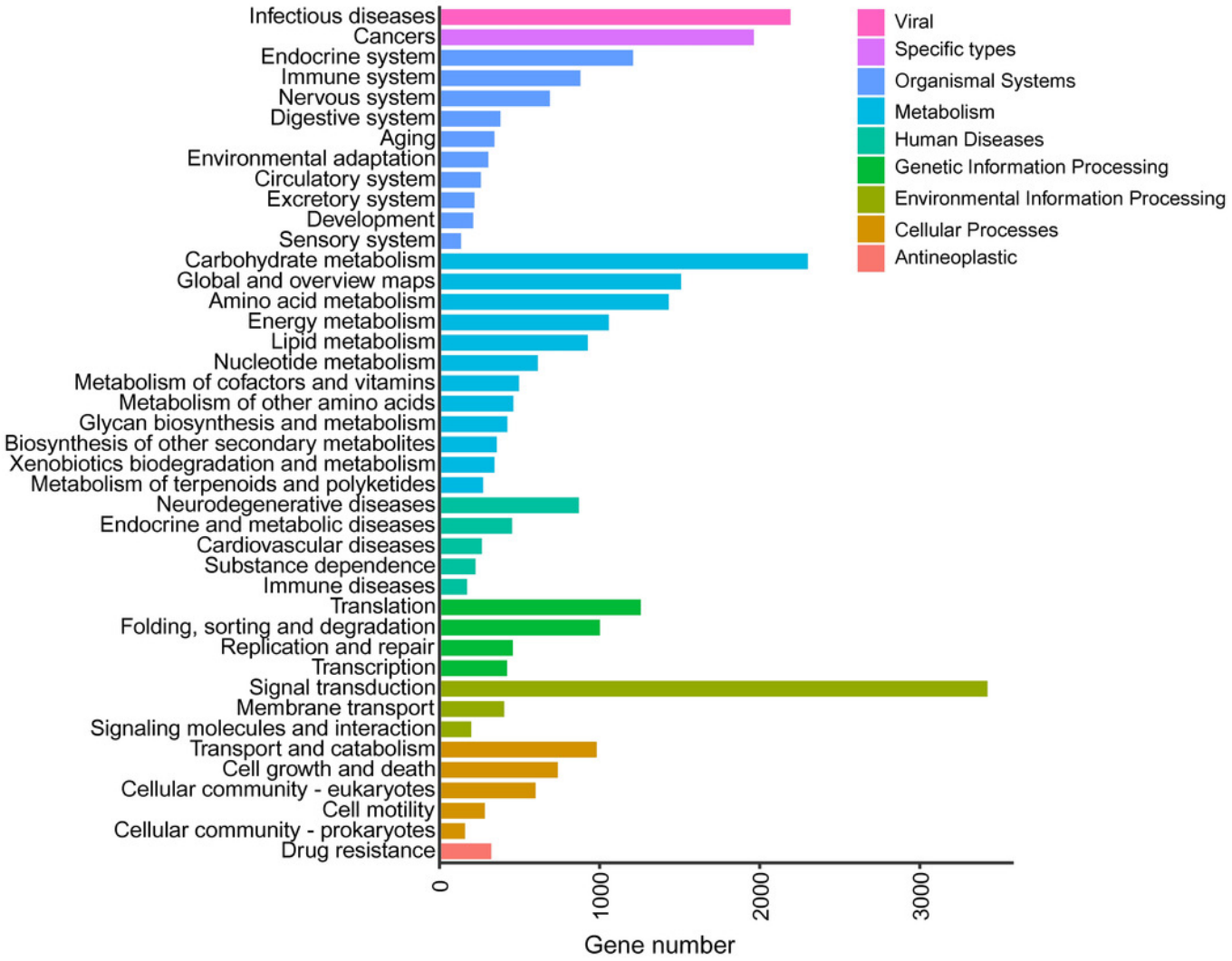

# Figure 4

DEGs identified between HJG and TN1.

A1 and A2 indicate three biological replicates of HJG and TN1 under NT; B1 and B2 indicate three biological replicates of HJG and TN1 under LT. the y-axis indicates the number of DEGs. The red block represents significant up-regulated genes and the turquoise block represents down-regulated genes.

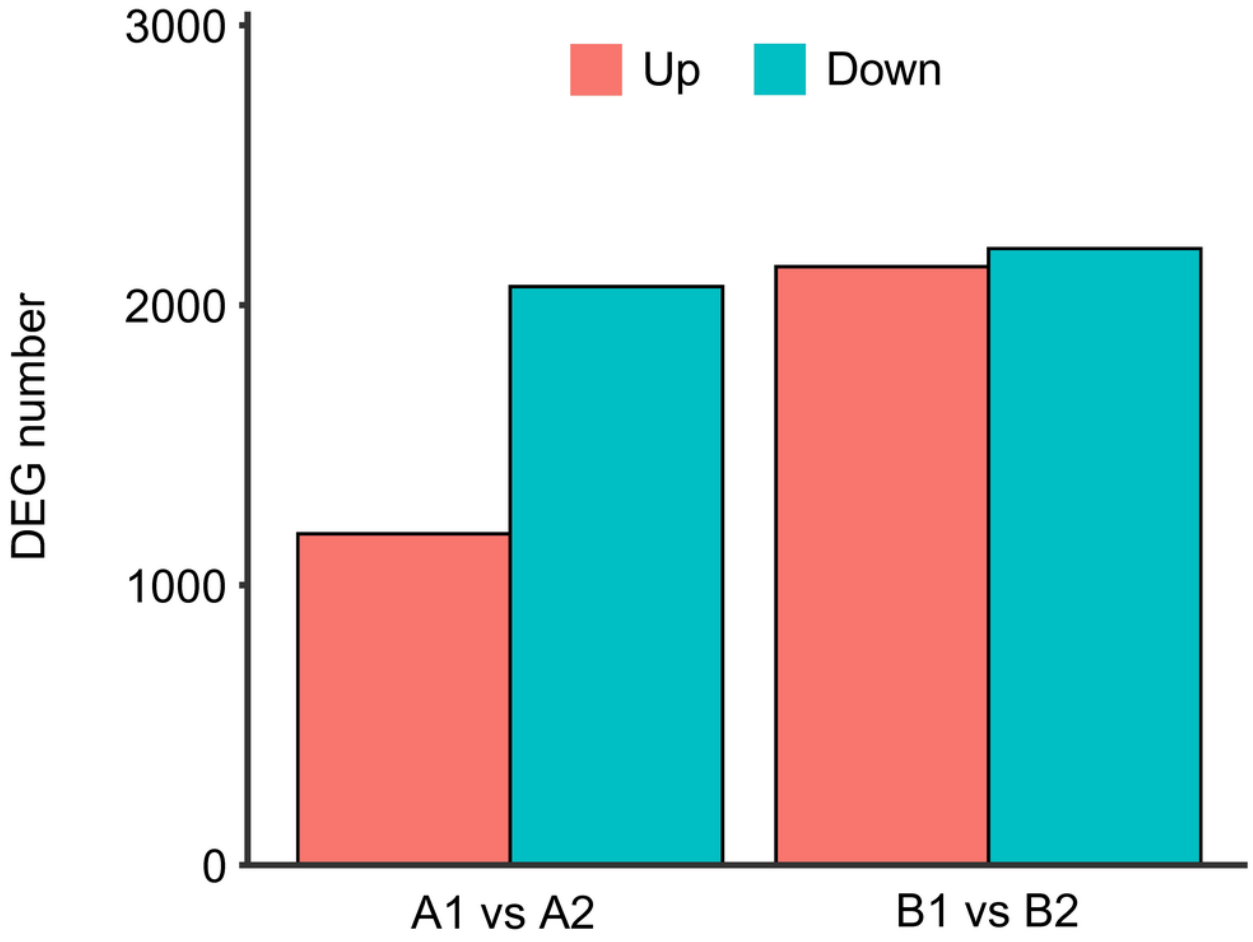

# Figure 5

Cluster analysis of DEGs patterns.

(a) A1 vs A2; (b) B1 vs B2. Red indicates that the gene is highly expressed in the sample; blue indicates lower expression, and the number label under the color bar at the upper left is the specific trend of the change of expression. The left is a dendrogram of gene clustering, and below is the name of the samples.

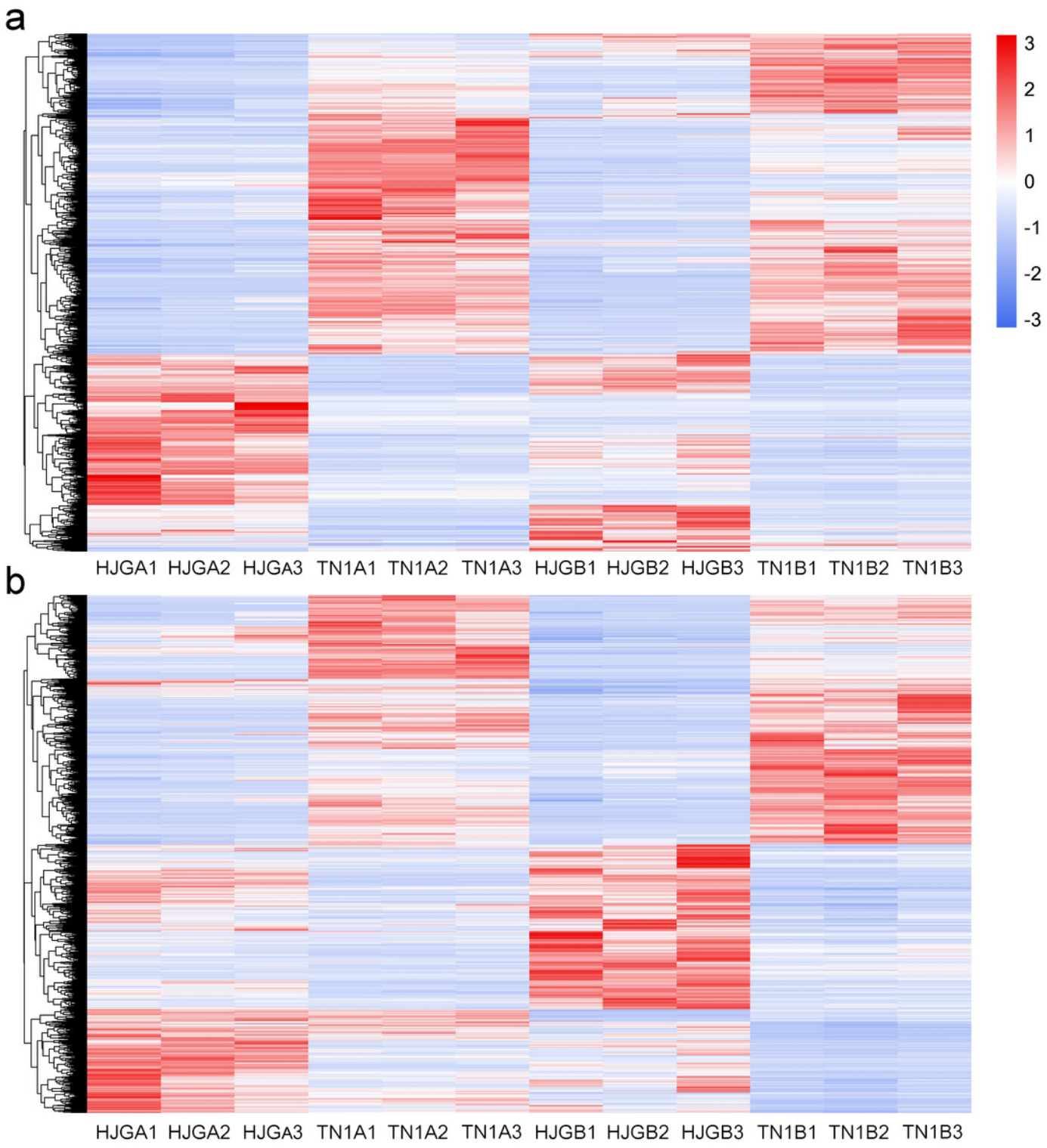
a
3
2
1
0
-1
-2
-3
HJGA1 HJGA2 HJGA3 TN1A1 TN1A2 TN1A3 HJGB1 HJGB2 HJGB3 TN1B1 TN1B2 TN1B3
b
HJGA1 HJGA2 HJGA3 TN1A1 TN1A2 TN1A3 HJGB1 HJGB2 HJGB3 TN1B1 TN1B2 TN1B3

# Figure 6

KEGG pathway enrichment of DEGs.

(a) A1 vs A2; (b) B1 vs B2. The left is the name of pathways, and below is the enrichment factor. The size of the dots indicate the number of genes in this pathway, and the color of the dots corresponds to different −log10(correct p value) ranges.

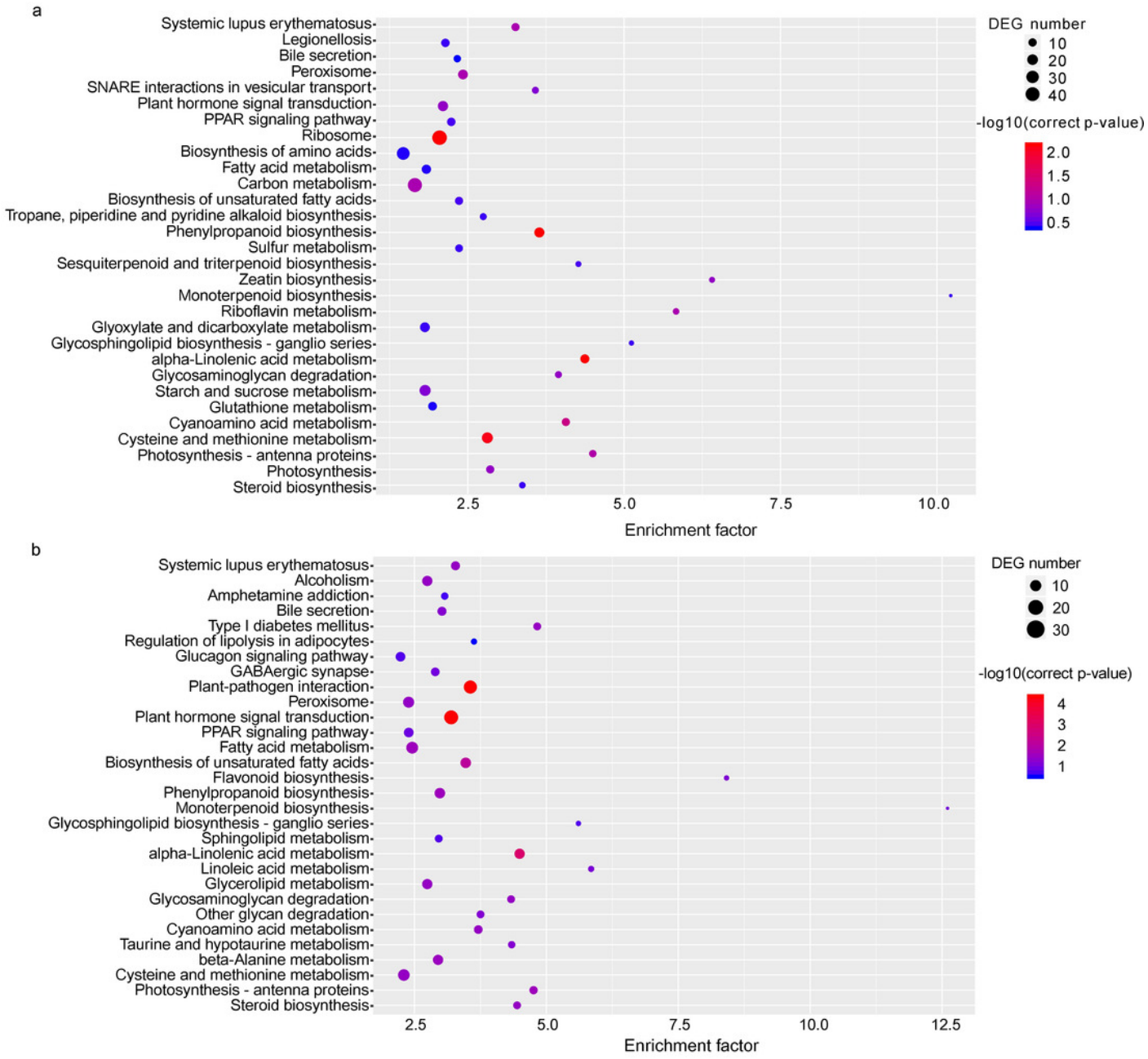
a
Systemic lupus erythematosus
Legionellosis
Bile secretion
Peroxisome
SNARE interactions in vesicular transport
Plant hormone signal transduction
PPAR signaling pathway
Ribosome
Biosynthesis of amino acids
Fatty acid metabolism
Carbon metabolism
Biosynthesis of unsaturated fatty acids
Tropane, piperidine and pyridine alkaloid biosynthesis
Phenylpropanoid biosynthesis
Sulfur metabolism
Sesquiterpenoid and triterpenoid biosynthesis
Zeatin biosynthesis
Monoterpenoid biosynthesis
Riboflavin metabolism
Glyoxylate and dicarboxylate metabolism
Glycosphingolipid biosynthesis - ganglio series
alpha-Linolenic acid metabolism
Glycosaminoglycan degradation
Starch and sucrose metabolism
Glutathione metabolism
Cyanoamino acid metabolism
Cysteine and methionine metabolism
Photosynthesis - antenna proteins
Photosynthesis
Steroid biosynthesis
2.5
5.0
7.5
10.0
Enrichment factor
DEG number
10
20
30
40
-log10(correct p-value)
2.0
1.5
1.0
0.5
b
Systemic lupus erythematosus
Alcoholism
Amphetamine addiction
Bile secretion
Type I diabetes mellitus
Regulation of lipolysis in adipocytes
Glucagon signaling pathway
GABAergic synapse
Plant-pathogen interaction
Peroxisome
Plant hormone signal transduction
PPAR signaling pathway
Fatty acid metabolism
Biosynthesis of unsaturated fatty acids
Flavonoid biosynthesis
Phenylpropanoid biosynthesis
Monoterpenoid biosynthesis
Glycosphingolipid biosynthesis - ganglio series
Sphingolipid metabolism
alpha-Linolenic acid metabolism
Linoleic acid metabolism
Glycerolipid metabolism
Glycosaminoglycan degradation
Other glycan degradation
Cyanoamino acid metabolism
Taurine and hypotaurine metabolism
beta-Alanine metabolism
Cysteine and methionine metabolism
Photosynthesis - antenna proteins
Steroid biosynthesis
2.5
5.0
7.5
10.0
12.5
Enrichment factor
DEG number
10
20
30
-log10(correct p-value)
4
3
2
1

# Figure 7

Thr heat map of DEGs.

(a) A1 vs A2; (b) B1 vs B2. The below is the name of the samples. Red indicates that the gene is highly expressed in the sample; blue indicates lower expression, and the number label under the color bar at the upper left is the specific trend of the change of expression.

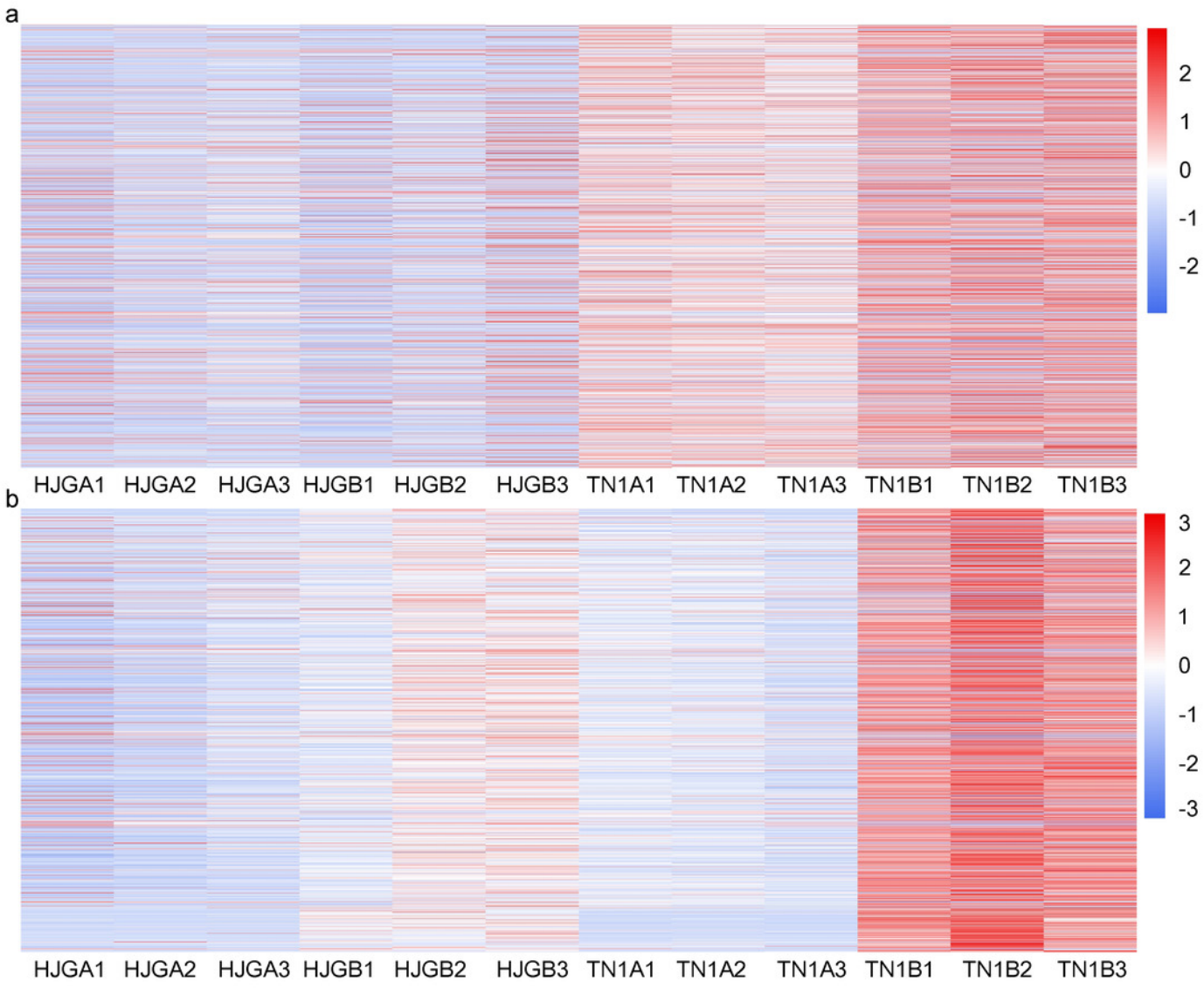

# Figure 8

KEGG pathway enrichment in brown module.

The x-axis below is the enrichment factor; the y-axis is the name of pathways. The size of the dots indicate the number of genes in this pathway, and the color of the dots corresponds to different −log10(correct p value) ranges.

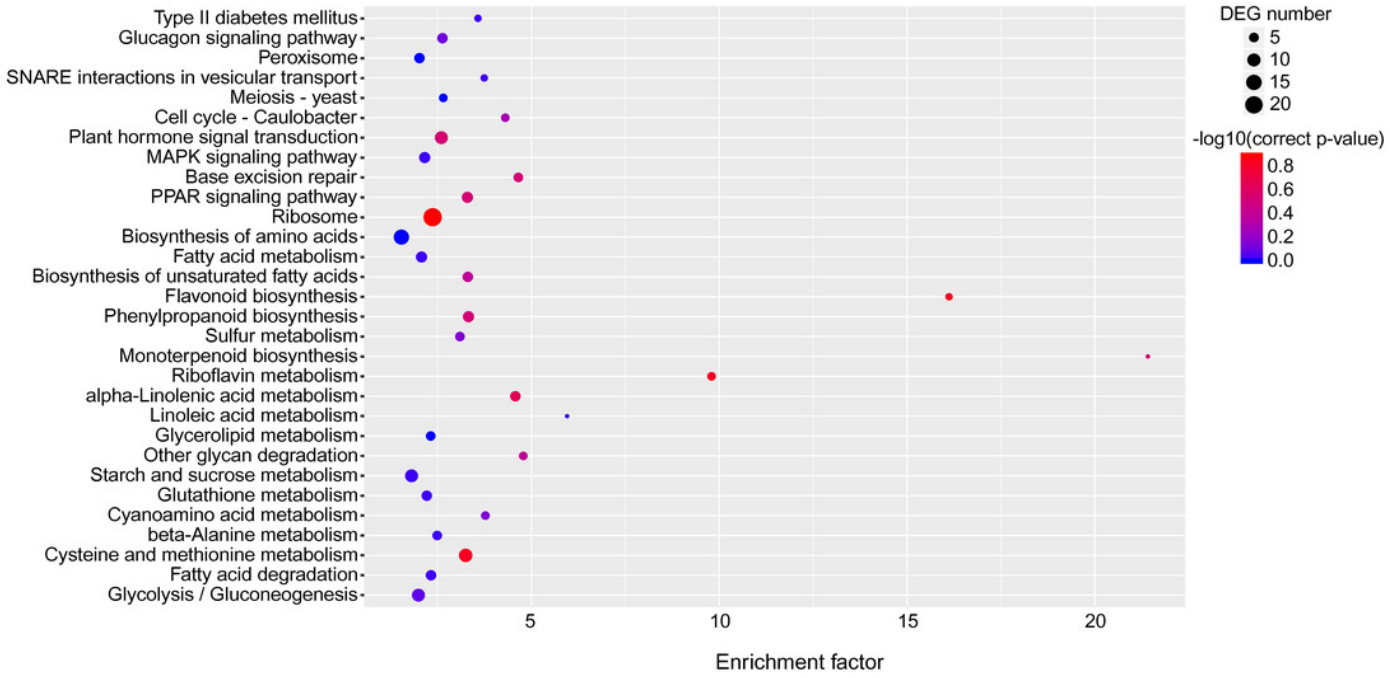

# Figure 9

KEGG pathway enrichment of yellow module.

The x-axis indicates the enrichment factor; the y-axis indicates the name of pathways. The size of the dots indicate the number of genes in this pathway, and the color of the dots corresponds to different −log10(correct p value) ranges.

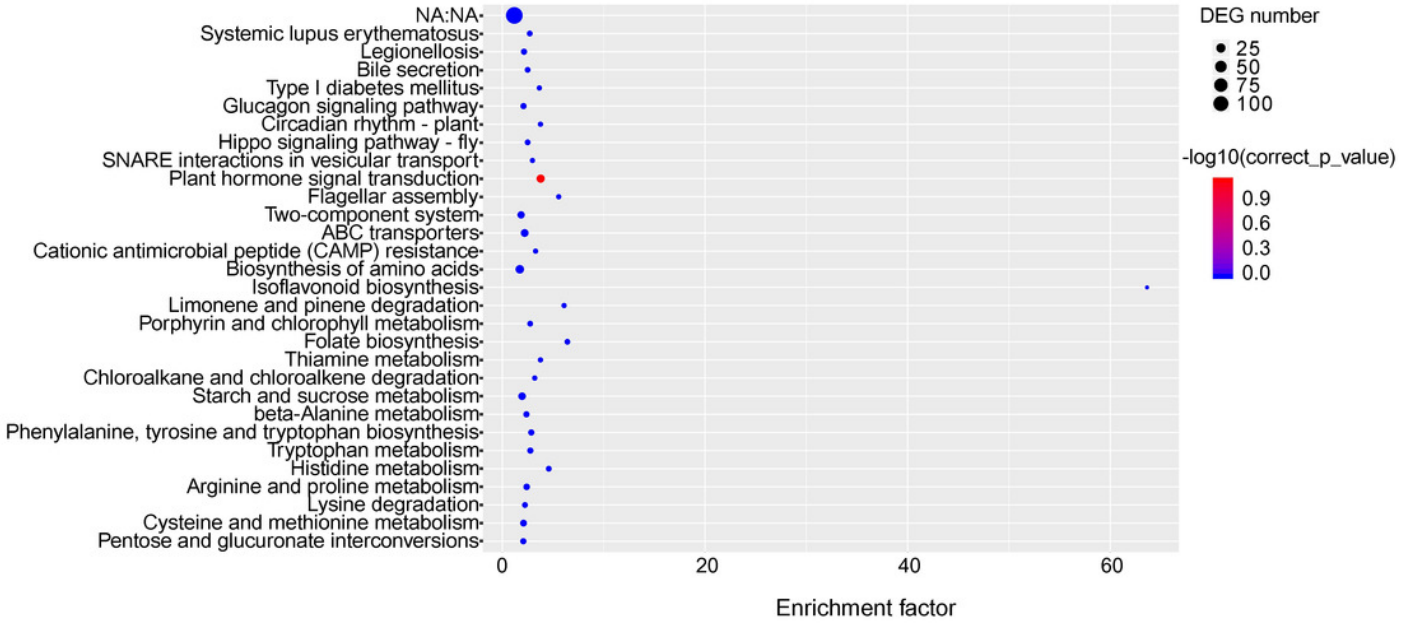

# Figure 10

Gene coexpression network related to cold stress.

(a) Gene co-expression network related tocold stress in brown module; (b) ene co-expression network related tocold stress in yellow module. Red dots represent the hube gene belonging to the co-expression network.

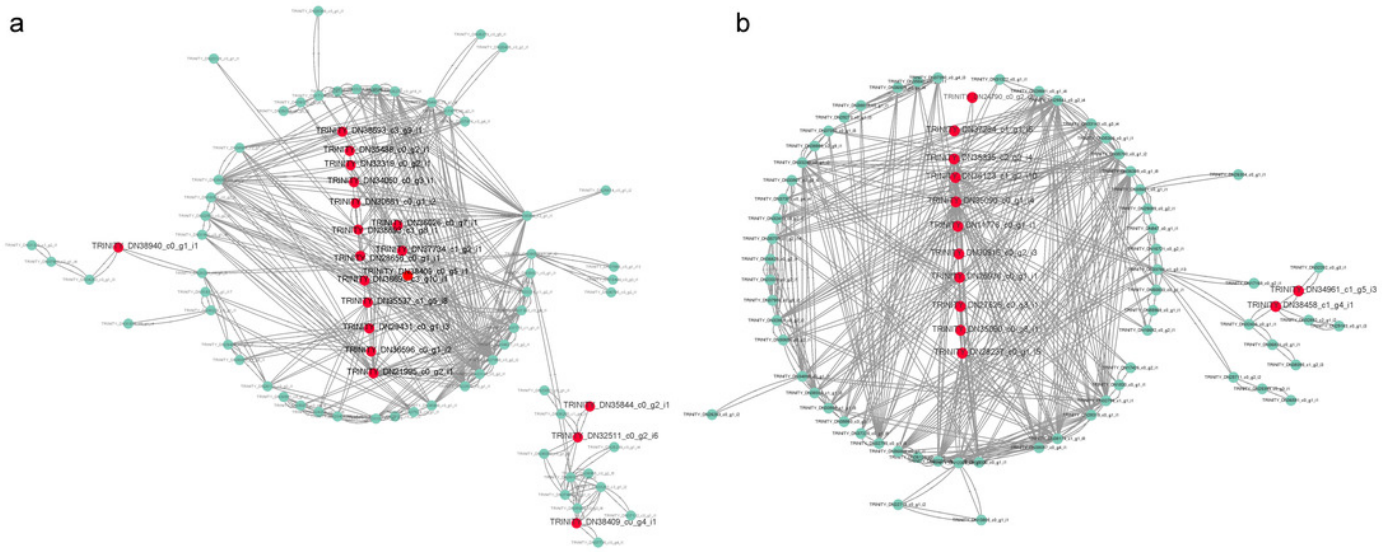

# Figure 11

Cold acclimation related genes were validated by qRT-PCR.

The blocks indicate the samples of HJG and TN1 using in RT-qPCR and RNA-seq under cold stress condition. Bars indicate standard deviations of three biological repetitions.